Improvement in the beam lifetime by means of an rf phase modulation at the KEK Photon Factory storage ring

Shogo Sakanaka,* Masaaki Izawa, Toshiyuki Mitsuhashi, and Takeshi Takahashi

Institute of Materials Structure Science, High Energy Accelerator Research Organization (KEK), 1-1 Oho, Tsukuba-shi, Ibaraki-ken, 305-0801 Japan

(Received 28 February 2000; published 10 May 2000)

In the 2.5-GeV Photon Factory storage ring at KEK, we have found that the beam lifetime can be improved by modulating the phase of an rf accelerating voltage at a frequency of 2 times the synchrotron oscillation frequency. By applying this phase modulation with a peak-to-peak amplitude of 3.2°, the beam lifetime could be improved, typically, from 22 to 36 h under a beam current of about 360 mA. At the same time, the longitudinal coupled-bunch instability could be considerably suppressed. The improvement in the beam lifetime can be explained as an improved Touschek lifetime, which was caused by a quadrupole-mode longitudinal oscillation of the stored bunches.

PACS numbers: 29.20.Dh, 29.27.Bd

I. INTRODUCTION

A long beam lifetime is one of the most important performances for synchrotron radiation sources. In the 2.5-GeV Photon Factory (PF) storage ring [1] at KEK, the beam lifetime had mainly been determined by the scattering process of the stored electrons with residual gas molecules in the vacuum chamber. After a large-scale reconstruction of the PF storage ring to the current low-emittance lattice [2,3], by which the beam emittance was reduced from 130 to 36 nm rad, the beam lifetime due to the Touschek effect became very important. This is also due to an excellent vacuum pressure (about 6×10^{-8} Pa[1] on the average under a stored current of 400 mA) that has been achieved in the PF storage ring. Under the present low-emittance optics, the estimated Touschek lifetime is comparable to, or shorter than, the lifetime due to the beam-gas scattering, even under routine multibunch operations. The principal parameters of the PF storage ring are given in Table I.

In the Photon Factory storage ring, we found that the beam lifetime could be improved by modulating the phase of the rf accelerating voltage at a frequency of 2 times the synchrotron oscillation frequency. At the same time, a longitudinal coupled-bunch instability, which has been observed under high beam currents, could be eased. Both of them were found to be beneficial to our operations. In order to clarify the beam dynamics under this phase modulation, we observed the longitudinal profiles of the bunches using a streak camera. We report on these experimental observations in Sec. II.

The observed improvement in the beam lifetime can be explained as being due to the Touschek lifetime, which is elongated by the following mechanism. By applying phase modulation at twice the synchrotron frequency, the longitudinal oscillations of the stored electrons are excited by a parametric resonance process. Because the electrons can execute two states of stable oscillations, the phases of which are opposite to each other, there arises a quadrupole-mode longitudinal oscillation of the bunches. This leads to a long bunch length on the average, which

TABLE I. Principal parameters of the Photon Factory storage ring under the present low-emittance optics (phase advance per cell: 105°).

Parameter	Symbol	Value
Beam energy	E	2.5 GeV
Stored current	I_0	770 mA max
Circumference	C	187.03 m
Horizontal betatron tune	ν_x	9.60
Vertical betatron tune	ν_y	4.28
Horizontal beam emittance	ϵ_x	3.6×10^{-8} mrad
Momentum compaction factor	α	0.0061
Natural energy spread	$(\sigma_\epsilon/E)_0$	7.3×10^{-4}
rf frequency	$f_{\rm rf}$	500.1 MHz
Harmonic number	h	312
Radiation loss per turn	U_0	399 keV
Longitudinal damping time	τ_ϵ	3.92 msec
Cavity gap voltage	V_c	1.7 MV (typically)
rf bucket height	$(\Delta E/E)_{\rm max}$	0.0122
Synchrotron oscillation frequency	f_s	22.7 kHz
Natural rms bunch length	σ_z	9.4 mm
Cavity shunt impedance ($= V_c^2/P_c$)	$R_{\rm sh}$	27.2 MΩ (in total)
Cavity unloaded Q	Q_0	39 000
Cavity loaded Q	Q_L	11 800

*Email address: shogo.sakanaka@kek.jp

[1]This pressure is about 3 times the average reading of vacuum gauges, which gives an estimated pressure on the beam path.

results in the long Touschek lifetime. We discuss this effect in Sec. III. Additionally, we give some discussions on the cure for the longitudinal coupled-bunch instability by this technique, although we have not fully understood its mechanism.

II. EXPERIMENTS

A. Beam lifetime and longitudinal coupled-bunch instability under phase modulation

The rf system of the PF storage ring is schematically shown in Fig. 1. Four 500-MHz rf cavities are used to produce an accelerating voltage. Each rf station comprises a 500-MHz rf cavity, a single 200-kW klystron, an rf distribution network, and low-level control circuits. The master 500-MHz rf signal is distributed into four signals, which then drive the four rf stations. Each rf phase of the klystron output is locked to the master rf by using a phase-lock loop. We installed an electric phase shifter just after the master rf generator. This allows us to modulate the phase of the master rf by an external control signal. Then, the klystron output waves of the four stations are modulated at the same time. In order that the cavity field can follow any modulation in the input rf wave, the bandwidth of the cavity (defined by the resonance frequency divided by a loaded Q value) should be comparable to, or wider than, the modulation frequency. Because the bandwidth of our cavity is about 42 kHz, the cavity field can follow the phase modulation up to about this frequency, with a certain amplitude and phase responses due to the cavity impedance.

Although excellent damped-accelerating cavities [4] are used in the PF storage ring, there arise many spectrum lines in a button-type electrode signal due to a longitudinal coupled-bunch instability above a beam current of about 100 mA. Since these spectrum lines do not correspond to any frequencies of the cavity higher order modes, we consider that the observed longitudinal instability is induced by some resonant structures in the vacuum components. This instability degrades the beam quality at high currents.

Kobayakawa [5] reported in 1984 that a small external phase modulation applied on the accelerating field could suppress a fluctuation in the beam size due to a longitudinal coupled-bunch instability. At that time, the frequency of the modulation was chosen to be very close to the synchrotron frequency. The first motivation of our experiment was to investigate whether a similar technique would be useful under the present operation, in which many of the parameters and components of the storage ring are very different from those in 1984.

Figure 2 shows the beam spectrum around one of the harmonics of the rf frequency when we modulated the rf phase at a frequency close to the synchrotron frequency. Beside the harmonic of the rf frequency, we can see both sideband signals which are apart from the main peak by once and twice the synchrotron frequency. This indicates that the bunches executed a synchrotron oscillation coherently in a dipole mode of oscillation (i.e., the center of each bunch oscillated longitudinally at the synchrotron frequency). In this case, we could observe only a slight suppression in the longitudinal coupled-bunch instability, even when we scanned the frequency and amplitude of the modulation. There was also little improvement in the beam lifetime.

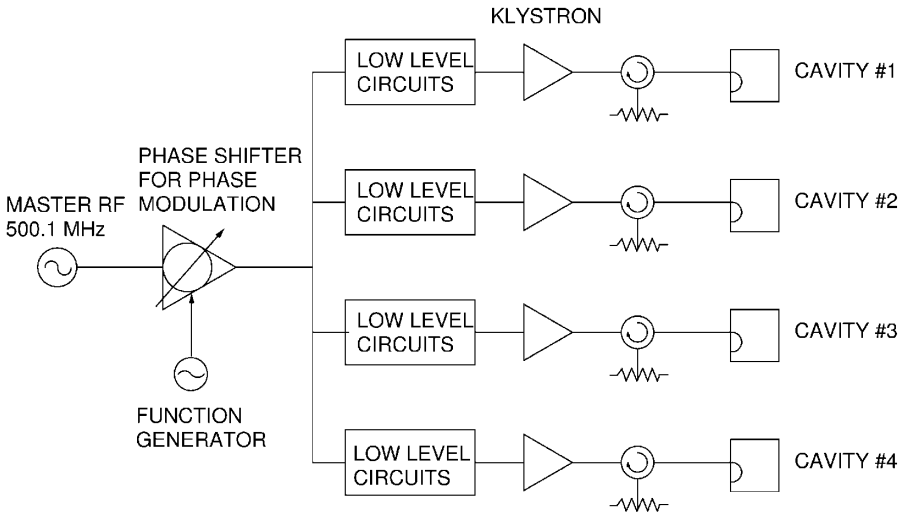

FIG. 1. Schematic diagram of the rf system for the PF storage ring. Four rf stations are used for beam acceleration. A fast phase shifter is used to modulate the phase of the master rf signal, which is distributed to the four rf stations.

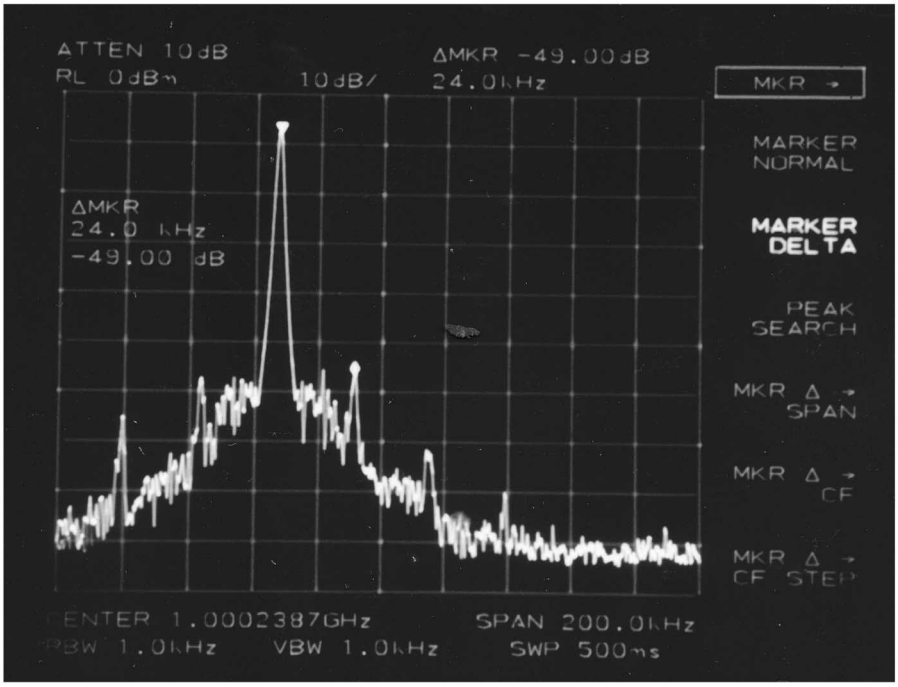

FIG. 2. Beam spectrum from a button-type electrode when we applied an rf phase modulation at a frequency of 23.8 kHz with a peak-to-peak modulation amplitude of 0.64°. The abscissa indicates the frequency (center frequency: 1.000 238 7 GHz; span: 200 kHz). The ordinate indicates the signal intensity in dB (10 dB/division). The beam current was 376 mA, which was filled in 280 bunches among 312 rf buckets. The main peak corresponds to the second harmonic of the rf frequency.

On the other hand, when we tuned the modulation frequency at about 2 times the synchrotron frequency, we obtained remarkable effects: (1) the beam lifetime was improved by a factor of about 1.6 and (2) the longitudinal coupled-bunch instability was considerably suppressed. A typical improvement in the beam lifetime is shown in Fig. 3. In this example, we obtained a beam lifetime of about 36 h under a beam current of about 360 mA by applying phase modulation, while the lifetime was about 22 h without the modulation. We discuss the mechanism of this improvement in Sec. III.

Another benefit gained by the phase modulation is shown in Figs. 4 and 5. Figure 4 shows our typical beam spectrum in which many spectrum lines due to the longitudinal coupled-bunch instability can be seen. When we applied the phase modulation, the spectrum changed as shown in Fig. 5; many spectrum lines were reduced in their level. This suggested that we could considerably suppress the longitudinal coupled-bunch instability by applying the phase modulation at twice the synchrotron frequency.

Figure 6 shows the beam spectrum in the vicinity of the second harmonic of the rf frequency when we applied phase modulation at this frequency. All of the other conditions, except for the modulation frequency, were the same as those in Fig. 2. We can see that the frequencies of the sidebands were apart from the second rf harmonic by twice the synchrotron frequency. This is a sign showing that the bunches executed the longitudinal oscillations coherently in a quadrupole mode of oscillation (i.e., the bunch length oscillated while keeping the center of the bunches).

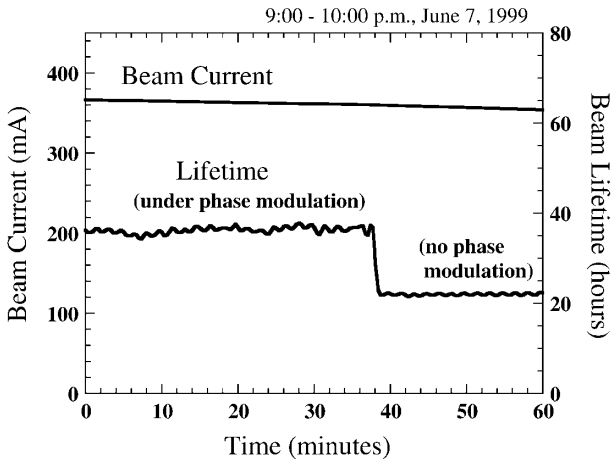

FIG. 3. Comparison of the beam lifetime (right-hand scale) with and without applying phase modulation. The modulation was initially on and was turned off at the time of 38 min. The frequency and the amplitude of the modulation were 48.1 kHz and 3.2° (peak to peak), respectively. The average ring pressure was 7.4×10^{-8} Pa with the modulation and 8.2×10^{-8} Pa without the modulation. The beam current (left-hand scale) is also shown.

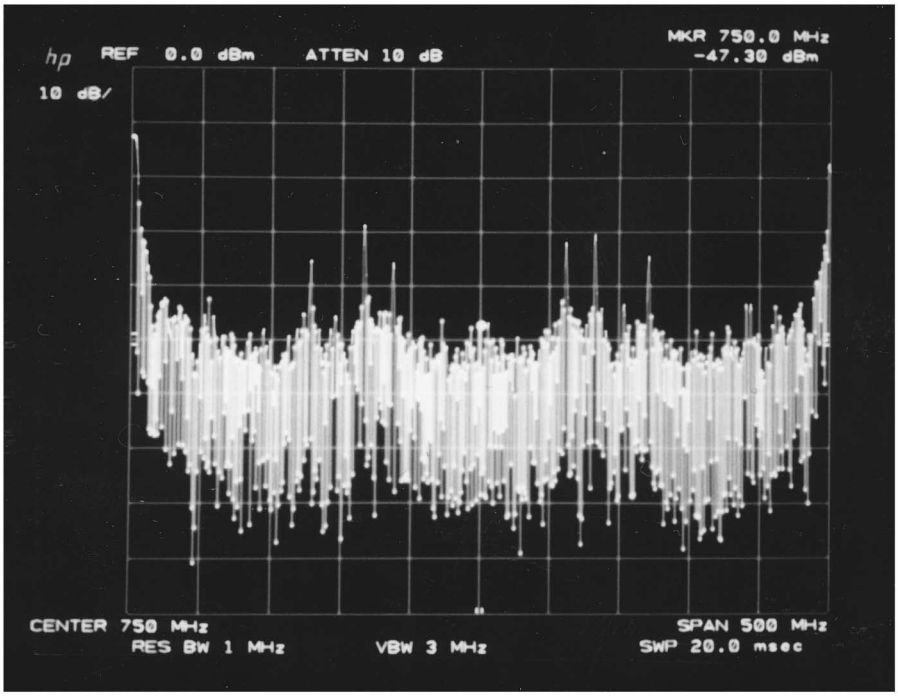

FIG. 4. Beam spectrum from the button-type electrode under a beam current of 256 mA with 280 bunches. No phase modulation was applied. Between the first harmonic (left-side peak) and the second harmonic (right-side peak) of the rf frequency there arose many spectrum lines due to the longitudinal coupled-bunch instability. The abscissa and ordinate show the frequency (center: 750 MHz; span: 500 MHz) and the signal intensity (10 dB/division), respectively.

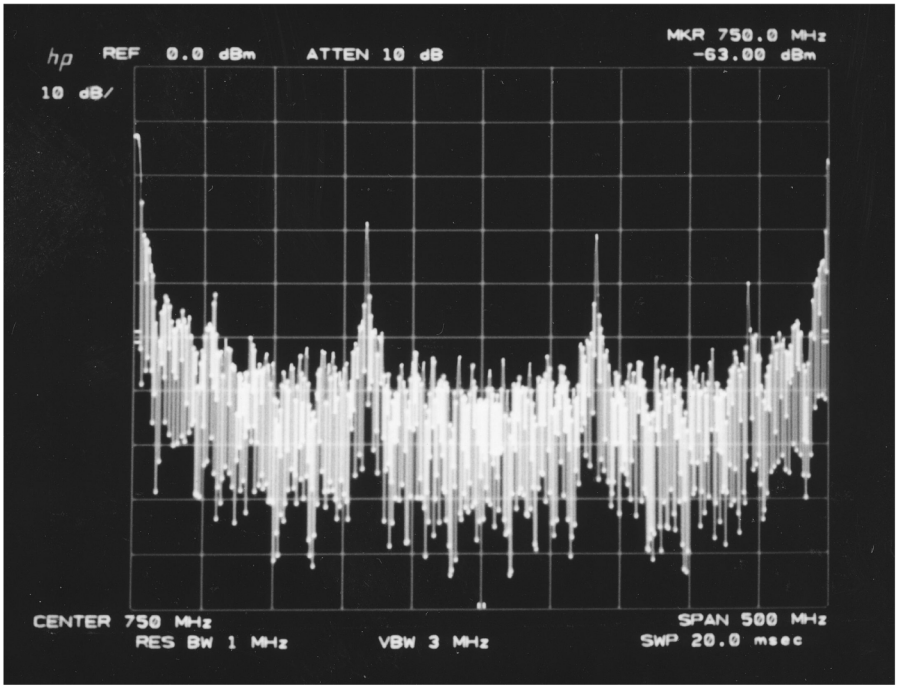

FIG. 5. Beam spectrum when phase modulation (47.4 kHz and 3.2° peak to peak) was applied. The beam current, the figure scales, and the other experimental conditions, except for the phase modulation, were the same as those in Fig. 4. The signal levels of many spectrum lines due to the longitudinal coupled-bunch instability were considerably reduced. Note that two peaks at frequencies of about 667 and 833 MHz are the harmonics of the revolution frequency, which appeared due to a fluctuation in the particle populations of the bunches.

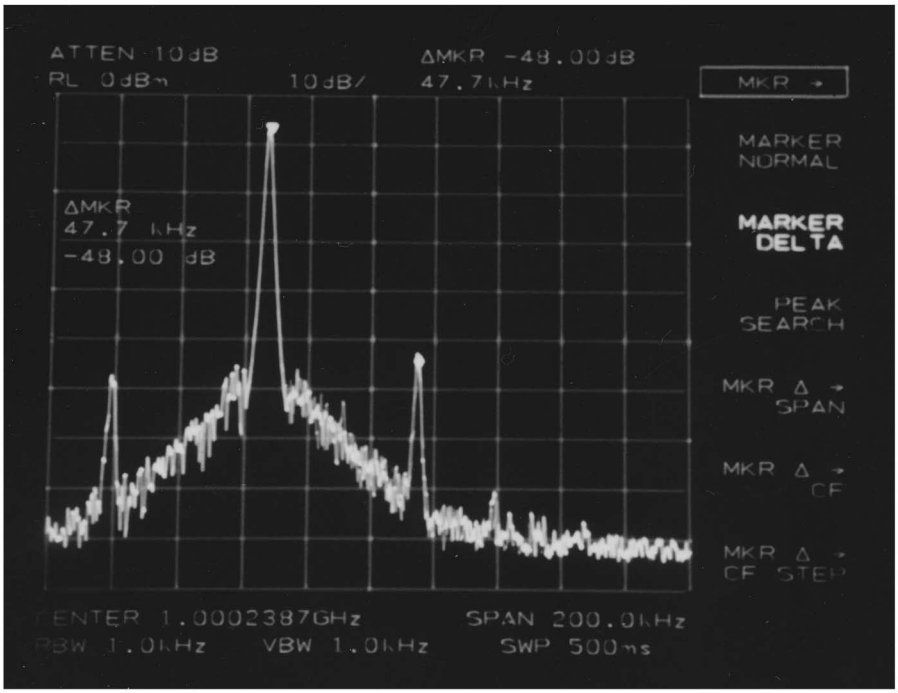

FIG. 6. Beam spectrum around the second harmonic of the rf frequency when we applied phase modulation at a frequency of 47.6 kHz with a peak-to-peak amplitude of 0.64°. The scales are the same as those in Fig. 2. The beam current was 376 mA with 280 bunches.

B. Observation of the longitudinal bunch profiles using a streak camera

In order to investigate the longitudinal beam dynamics under phase modulation, we observed the longitudinal profiles of the bunches. Visible synchrotron light from the stored bunches was extracted from bending magnet No. 27. The light was then filtered by both a bandpass filter and a dichroic polarizer (which selected the σ-polarization component), in order to maximize the temporal resolution of the optical system. The light was finally focused on the entrance slit of a streak camera (Hamamatsu C5680 with a synchroscan unit M5675 and a dual time-base unit M5679). This streak camera can measure the intensity variations in the light with a very high resolution of 2 ps. We applied a dual time-base measurement technique; photoelectrons emitted in a streak tube were swept very fast in the vertical direction, while applying an auxiliary slow-sweep signal in the horizontal direction. Thus, the fast intensity variation of the incident light was shown

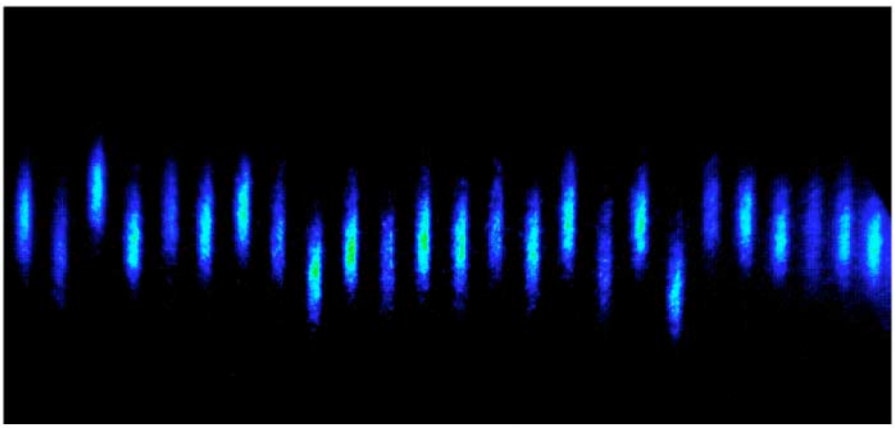

FIG. 7. (Color) Longitudinal profile of the stored bunches without applying phase modulation. This image was obtained from a dual time-base measurement using a streak camera. The vertical axis shows a fast variation of the incident synchrotron light, while the images from many scans are separated in the horizontal axis. Longitudinal profiles of every four bunches are shown separately. Vertical full scale, 600 ps; horizontal full scale, 200 ns. Beam current was 399 mA in 280 bunches.

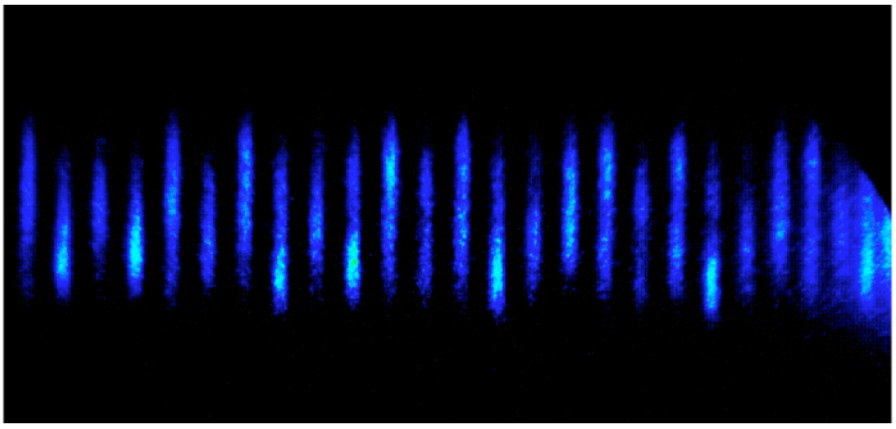

FIG. 8. (Color) Longitudinal profile of every fourth bunch under the rf phase modulation. The frequency and the amplitude of the modulation were 48.1 kHz and 3.2° (peak to peak), respectively. The beam current was 388 mA. All the other conditions were the same as those in Fig. 7. Vertical full scale: 600 ps; horizontal full scale: 200 ns.

along the vertical axis, while many images obtained from multiple scans were separately shown along the horizontal axis. This allowed us to observe the longitudinal profiles of the many bunches at the same turn.

The measured profile of the bunches without applying the phase modulation is shown in Fig. 7. Since we applied the main sweep signal at a frequency of 125 MHz (one-fourth of the rf frequency), we could observe the longitudinal profile of every fourth bunch. We can see in Fig. 7 that the centers of the bunches were located back and forth, which indicated a longitudinal coupled-bunch oscillation.

Figure 8 shows the result of a similar measurement when we applied the rf phase modulation at the frequency of twice the synchrotron frequency. We can see from this figure that (1) the bunches were lengthened longitudinally on the average, (2) some of the bunches showed a longitudinal distribution having double peaks, and (3) the amplitude of the longitudinal coupled-bunch oscillation was reduced. These observations suggested that the bunches executed longitudinal oscillations in a quadrupole mode of oscillation and that the average length of the bunches was elongated by applying phase modulation.

The effect of the phase modulation on the longitudinal coupled-bunch instability is demonstrated in Figs. 9 and 10. Both figures show the results similar to the above-mentioned measurement, but with a different horizontal scale (1 μs full scale). Figure 9 is the longitudinal profile of the bunches under no phase modulation. We can clearly see winding in the longitudinal position of the bunches due to the longitudinal coupled-bunch oscillation. On the other hand, the measurement result under phase modulation (Fig. 10) shows that the coupled-bunch oscillation was remarkably suppressed by the phase modulation.

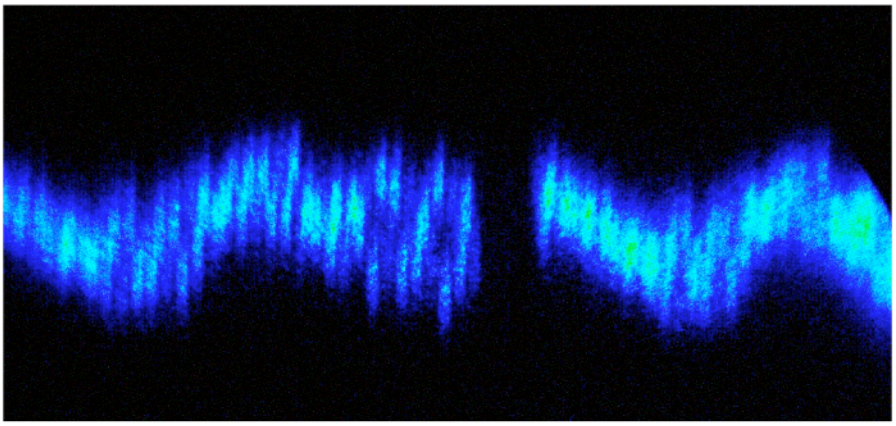

FIG. 9. (Color) Longitudinal profile of the bunches without applying phase modulation. Vertical full scale: 600 ps; horizontal full scale: 1 μs. The profiles of every four bunches were measured over about 1.6 circulations of the beam (revolution time: 0.624 μs). The beam current was about 396 mA with 280 bunches. The gap (empty buckets) of about 10% of the ring can be seen in the figure.

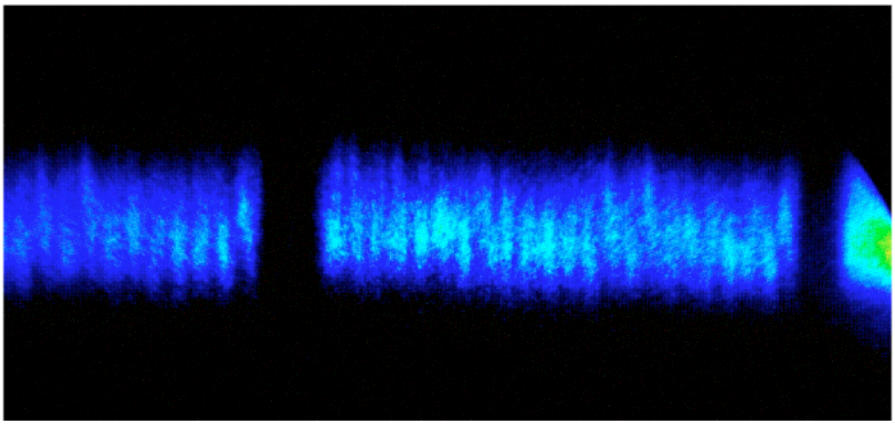

FIG. 10. (Color) Longitudinal profile of the bunches under phase modulation (48.1 kHz, 3.2° peak to peak). Vertical full scale, 600 ps; horizontal full scale, 1 μs. The beam current was 383 mA. All other conditions, except for the phase modulation and the small difference in the beam current, were kept the same as those in Fig. 9.

III. DISCUSSIONS

A. Single-particle dynamics under phase modulation

We consider the longitudinal motion of a single electron under phase modulation. In order to simplify the treatment, we assume here that the rf field in the cavities is modulated similarly as the input rf, by which the response due to the cavity impedance is neglected. We also do not consider the beam-loading effect. Let τ be the longitudinal time advance of an electron away from its synchronous position and δ be the relative energy deviation from that of the synchronous particle. The equations of motion for the electron are given by

$$\frac{d\tau}{dt} = -\alpha\delta\,, \tag{1}$$

and

$$\frac{d\delta}{dt} = \frac{eV_c\cos(\phi_0 - \omega\tau + \phi_m) - U_0}{T_0E_0} - 2\gamma_\epsilon\delta\,, \tag{2}$$

where α is the momentum compaction factor, e is the elementary charge, V_c is the cavity gap voltage, T_0 is the revolution time, E_0 is the energy of the synchronous particle, U_0 is the radiation loss per turn for the synchronous particle, ϕ_0 is the synchronous phase ($\cos\phi_0 = U_0/eV_c$), ω is the angular rf frequency, and γ_ϵ is the radiation damping rate [$= \frac{1}{2T_0}(\frac{dU}{dE})_{E0}$]. Here the phase modulation is described by ϕ_m. We are interested in the situation where the rf phase is modulated at the frequency of twice the synchrotron frequency,

$$\phi_m = \phi_{m0}\cos(2\omega_s t)\,, \tag{3}$$

where ϕ_{m0} is the modulation amplitude and ω_s is the unperturbed synchrotron frequency, which is given by

$$\omega_s = \sqrt{\frac{\alpha\omega eV_c\sin\phi_0}{T_0E_0}}\,. \tag{4}$$

In the cases that both ϕ_m and $\omega\tau$ are small ($\phi_m, \omega\tau \ll 1$), we can make the following approximation in Eq. (2):

$$\cos(\phi_0 - \omega\tau + \phi_m) \approx \cos\phi_0 - \phi_m\sin\phi_0 + (\sin\phi_0 + \phi_m\cos\phi_0)\omega\tau\,. \tag{5}$$

Combining this with Eqs. (1)–(3), we obtain the following equation of motion for τ:

$$\frac{d^2\tau}{dt^2} + 2\gamma_\epsilon\frac{d\tau}{dt} + \omega_s^2\{1 + \epsilon\cos(2\omega_s t)\}\tau = \frac{\omega_s^2\phi_{m0}}{\omega}\cos(2\omega_s t)\,, \tag{6}$$

where ϵ is a small dimensionless number given by

$$\epsilon = \phi_{m0}\cot\phi_0\,. \tag{7}$$

Equation (6) is essentially the Mathieu equation, which describes the motion of an oscillator that is driven by some change in its parameter at a frequency of twice the eigenfrequency. The additional second term in the left-hand side of Eq. (6) describes the damping effect due to synchrotron radiation. The other additional term in the right-hand side describes a forced driving term to the oscillator. Since the frequency of this driving force ($2\omega_s$) is far from the eigenfrequency (ω_s), this term has little effect on the electron motion. We can thus reduce the equation to

$$\frac{d^2\tau}{dt^2} + 2\gamma_\epsilon\frac{d\tau}{dt} + \omega_s^2\{1 + \epsilon\cos(2\omega_s t)\}\tau = 0\,. \tag{8}$$

This equation holds under small oscillation amplitudes.

We can obtain an approximate solution of this equation by applying an averaging method, as can be found in the literature [6,7]. We expect an approximate solution in form

$$\tau(t) = a(t)\sin(\omega_s t) + b(t)\cos(\omega_s t)\,, \tag{9}$$

with the binding condition

$$\dot{a}(t)\sin(\omega_s t) + \dot{b}(t)\cos(\omega_s t) = 0\,. \qquad (10)$$

Here, $a(t)$ and $b(t)$ are assumed to be slowly varying functions of time. Substituting them into Eq. (8), and averaging the equations over one synchrotron period, yields the following approximate equations for $a(t)$ and $b(t)$:

$$\dot{a} = -\gamma_\epsilon a - \frac{\epsilon\omega_s}{4} b, \qquad \dot{b} = -\gamma_\epsilon b - \frac{\epsilon\omega_s}{4} a\,. \qquad (11)$$

From their solution, we obtain an approximate solution for τ,

$$\tau(t) = e^{-\gamma_\epsilon t}\left\{C_1 e^{-\alpha_g t}\cos\left(\omega_s t - \frac{\pi}{4}\right) + C_2 e^{\alpha_g t}\cos\left(\omega_s t - \frac{3\pi}{4}\right)\right\}, \qquad (12)$$

where α_g gives the growth rate of the synchrotron oscillation which is caused by the phase modulation,

$$\alpha_g = \frac{\omega_s \phi_{m0}\cot\phi_0}{4}\,. \qquad (13)$$

The above constants, C_1 and C_2, are determined by the initial condition.

It can be seen from Eq. (12) that the synchrotron oscillation grows exponentially if the modulation amplitude (ϕ_{m0}) is larger than a certain threshold, in which case the growth rate exceeds the radiation damping rate. Even in such a case, the growth will finally stop at some saturation amplitude where the nonlinear characteristic of the original equations becomes dominant. Since the sign of the constant C_2 is determined arbitrarily by the initial condition, an asymptotic solution at the saturation will be given by

$$\tau \sim \pm\tau_{\rm sat}\cos\left(\omega_s t - \frac{3\pi}{4}\right), \qquad (14)$$

where $\tau_{\rm sat}$ is a saturation amplitude. Each electron will take one of the above stable oscillations at saturation.

B. Simulations

For large-amplitude oscillations, the nonlinear characteristic of the original equations, (1) and (2), becomes important. We investigated this situation by a tracking simulation. In this simulation, the motion of a single particle under the phase modulation was calculated over 30 000 turns, based on Eqs. (1) and (2). The result is shown in Fig. 11, where the parameters of the PF storage ring (in Table I) were used. It can seen from the figure that (1) the synchrotron oscillation initially grows exponentially and (2) the oscillation amplitude finally reaches saturation. These features are just those expected in Sec. III A. It can be read from Fig. 11 that the initial growth rate is about 320 s^{-1}. This roughly agrees with an analytical prediction of $(\alpha_g - \gamma_\epsilon) \sim 200\ s^{-1}$ for the net growth rate. Figure 12 shows the tracks of the motion under saturation during the last 100 turns. At saturation, the trace of the motion is largely deformed from an ellipse due to phase modulation.

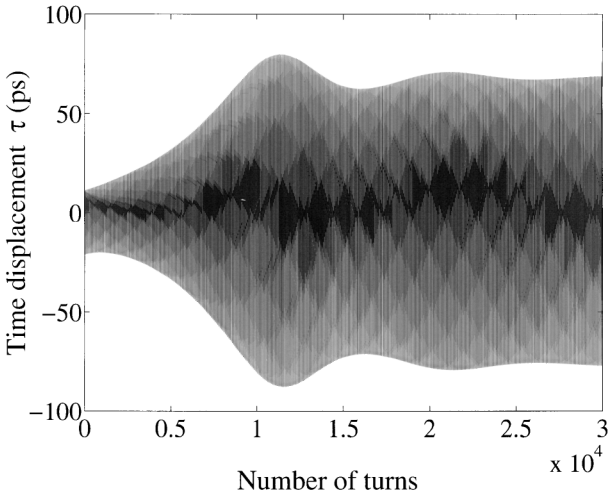

FIG. 11. Simulation result of the longitudinal single-particle motion under phase modulation. The time displacement (τ) is shown against the number of turns. Assumed $f_{\rm mod} = 45.36$ kHz (2 times the synchrotron frequency) and $\phi_{m0} = 0.052$ rad (6° peak to peak), where $f_{\rm mod}$ and ϕ_{m0} are the phase-modulation frequency and the modulation amplitude, respectively. All other parameters are taken from Table I. Initial condition: $\tau = 10$ ps, $\delta = 0$.

Furthermore, the behavior of the stored bunch under phase modulation was investigated by a multiparticle tracking simulation. In this calculation, a single bunch was modeled by using 1000 macroparticles. In addition to

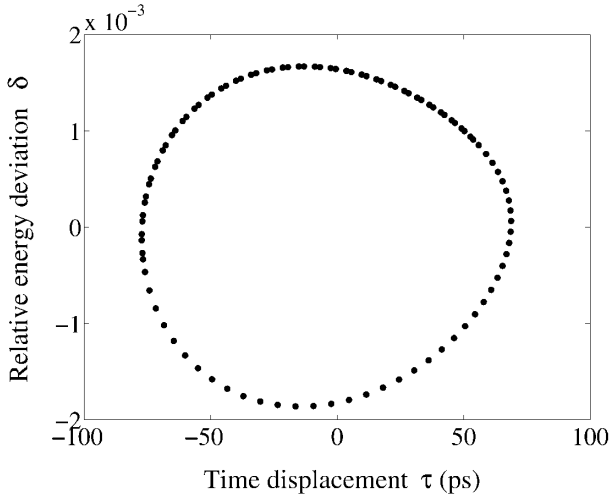

FIG. 12. Phase-space plot of the single-particle motion under the saturation. The closed circles indicate the tracks of the motion during the last 100 turns in the 30 000 turns. The phase modulation with $f_{\rm mod} = 45.36$ kHz and $\phi_{m0} = 0.052$ rad was assumed.

Eqs. (1) and (2), we took account of the following effects: (i) the radiation excitation, (ii) the cavity response to the modulated rf, and (iii) the beam-loading effect. We first describe how these effects were treated in the simulation.

In order to introduce the radiation excitation, we added a random quantity (r) in calculating the change in the δ per revolution, which describes the fluctuation in the radiation loss. The probability distribution for the r was assumed to be a Gaussian distribution having the following characteristics [8]:

$$\langle r \rangle = 0, \qquad \langle r^2 \rangle = \frac{4T_0}{\tau_\epsilon}\left(\frac{\sigma_\epsilon}{E}\right)_0^2, \tag{15}$$

where τ_ϵ is the radiation damping time, $(\sigma_\epsilon/E)_0$ is the natural energy spread, and $\langle\,\rangle$ denotes the average over ensembles.

Next, the cavity response to the phase modulation was treated as follows. Suppose that the phase of an input rf to the cavity is modulated as

$$\phi_m(t) = \phi_{m0}\cos(\omega_m t), \tag{16}$$

where ω_m is the angular modulation frequency. Then the input rf is represented by the generator current,

$$\tilde{i}_g = i_{g0}e^{i(\omega t+\theta+\phi_m)} = i_{g0}e^{i\theta}\sum_{n=-\infty}^{\infty} i^n J_n(\phi_{m0})e^{i(\omega+n\omega_m)t}, \tag{17}$$

with

$$i_{g0} = \sqrt{\frac{16\beta P_g}{R_{\rm sh}}}. \tag{18}$$

Here, θ represents an appropriate phase offset, ω is the angular rf frequency, $J_n(x)$ is the Bessel function of the first kind, $R_{\rm sh}$ is the cavity shunt impedance (defined by V_c^2/P_c, where P_c is the dissipated power), β is the cavity coupling coefficient, and P_g is the available power from the generator. The cavity loaded impedance for the frequency ω' is given by

$$\tilde{Z}_L(\omega') = \frac{\frac{R_{\rm sh}}{2(1+\beta)}}{1 + jQ_L(\frac{\omega'}{\omega_0} - \frac{\omega_0}{\omega'})}, \tag{19}$$

where ω_0 and Q_L are the cavity angular resonant frequency and the loaded Q value, respectively. Then, the generator-induced cavity voltage is given by

$$\tilde{V}_g = i_{g0}e^{i\theta}\sum_{n=-\infty}^{\infty} i^n J_n(\phi_{m0})\tilde{Z}_L(\omega + n\omega_m)e^{i(\omega+n\omega_m)t}. \tag{20}$$

The actual generator voltage is given by the real part of $\tilde{V}_g$. Note that only three terms for $n = 0$ and $n = \pm 1$ are sufficient in Eq. (20) if the ϕ_{m0} is sufficiently small.

The beam-loading effect [9] under the stored beam is incorporated by considering both the cavity detuning and the beam-induced voltage. In order to minimize the required generator power under the beam current, the cavity resonant frequency is usually detuned from the rf frequency so as to give the following optimum tuning angle:

$$\tan\psi_{\rm opt} = -\frac{I_0 R_{\rm sh}\sin\phi_0}{V_c(1+\beta)}. \tag{21}$$

Here, the tuning angle is defined by

$$\tan\psi = -Q_L\left(\frac{\omega}{\omega_0} - \frac{\omega_0}{\omega}\right). \tag{22}$$

We took account of this detuning in the simulation. Then, the cavity voltage is given by the vector sum of the generator-induced and a beam-induced voltages,

$$\tilde{V}_c = \tilde{V}_g + \tilde{V}_b. \tag{23}$$

The calculation of the beam-induced voltage $\tilde{V}_b$ can be carried out, in principle, by summing up the voltages induced by every macroparticle at every turn. In order to save the calculation time needed, we approximated this process by the following steps:

(i) As an initial condition for the beam-induced voltage, the voltage under the stable condition is assumed:

$$(\tilde{V}_b)_0 = \frac{I_0 R_{\rm sh}}{1+\beta}\cos\psi e^{i\psi}. \tag{24}$$

(ii) At every bunch passage, the bunch induces the following voltage in the cavity:

$$-2k_0 q_b \exp(-\omega_0^2\sigma_\tau^2/2), \tag{25}$$

where k_0 is the loss parameter of the accelerating mode, q_b is the bunch charge, and σ_τ is the rms bunch length in time. At the same time, every particle in the bunch is decelerated by the following voltage:

$$-k_0 q_b \exp(-\omega_0^2\sigma_\tau^2). \tag{26}$$

(iii) Between the bunch passages during a time duration Δt, the $\tilde{V}_b$ oscillates freely. This is represented by multiplying the $\tilde{V}_b$ by the following factor:

$$\exp\left(i\omega_0\Delta t - \frac{\omega_0\Delta t}{2Q_L}\right). \tag{27}$$

The above procedure is a good model provided that the rf wavelength is much longer than the bunch length.

Incorporating all of the above effects, we carried out multiparticle tracking simulations. The results are shown in Figs. 13–15. The first figure (Fig. 13) shows the distribution of the particles after about 30 000 turns for the case that the rf phase is modulated. The assumed parameters for this calculation (beam current, 360 mA; modulation frequency, 45.36 kHz; modulation amplitude, 3.2° peak to peak) are comparable to the experimental conditions in the case of Fig. 3. The small difference in the modulation frequency is due to a small discrepancy in the synchrotron frequency under the experiment (about 23.7 kHz) and under the simulation (about 22.7 kHz). The second simulation result with no phase modulation is shown in Fig. 14 as a reference. Both figures show that the particles are distributed in phase space due

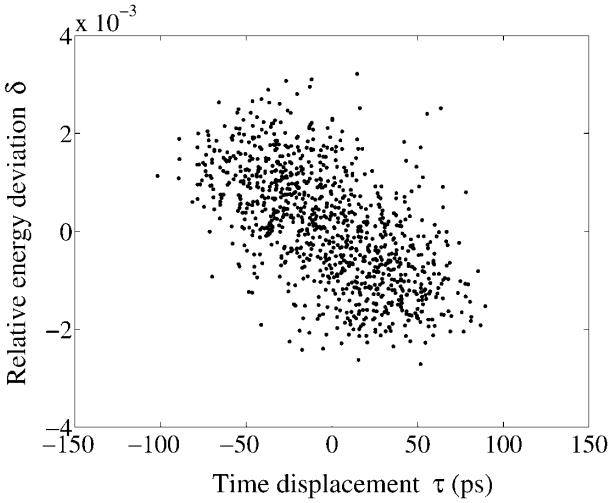

FIG. 13. Distribution of the particles under phase modulation at a high beam current ($I_0 = 360$ mA). The result of the multiparticle tracking simulation after about 30 000 turns is shown, in which a single bunch is modeled by using 1000 macroparticles. Each dot in the longitudinal phase space represents a macroparticle. The following parameters were used for the calculation: $f_{\mathrm{mod}} = 45.36$ kHz, $\phi_{m0} = 0.028$ rad (3.2° peak to peak), and other parameters are taken from Table I. Note that each particle goes around the center of the figure with a period of the synchrotron oscillation.

to the radiation excitation. However, in the first case (Fig. 13), the particles tend to gather around the two positions where the synchrotron oscillation induced by the phase modulation is most stable. Since these groups of particles execute synchrotron oscillations having opposite signs, the bunch length oscillates at twice the synchrotron frequency while the center of the bunch is kept still. This

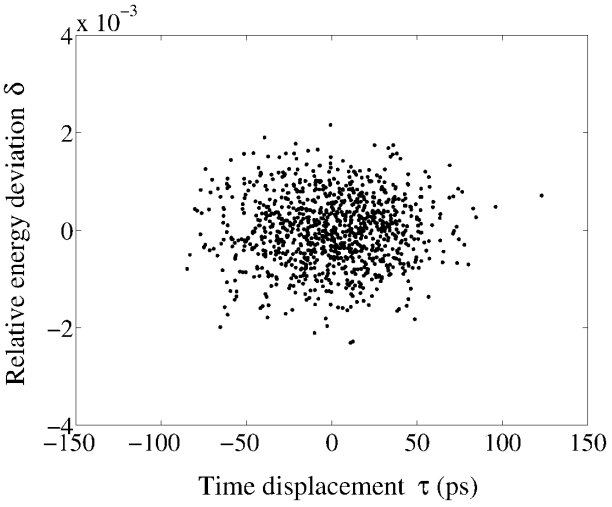

FIG. 14. Distribution of the particles under no phase modulation. The result of tracking after about 30 000 turns is shown. The beam current and the other parameters are the same as those in Fig. 13.

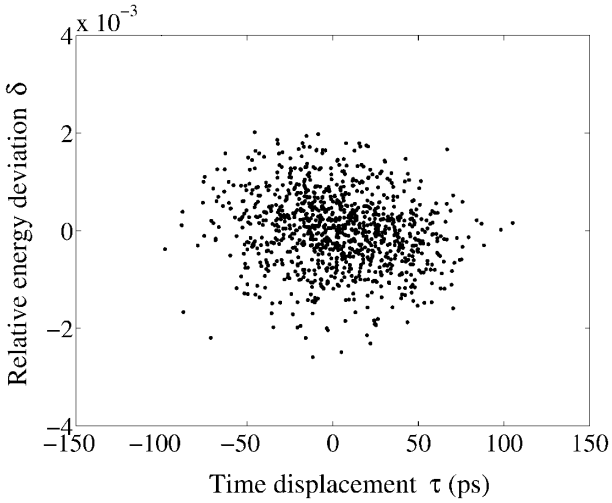

FIG. 15. Distribution of the particles under phase modulation, but with a low beam current of 1 mA. All other parameters are the same as those in Fig. 13.

oscillation of the bunch is considered to be a quadrupole mode of oscillation.

It is worth noting that the excitation of the longitudinal quadrupole oscillation is considerably enhanced by the beam-loading effect. This is demonstrated by the third simulation result (Fig. 15). This figure shows the simulation result for a low beam current of 1 mA, while keeping the other parameters the same as those in Fig. 13. Under this low current, the excitation of the quadrupole oscillation is considerably small. This dependence of the

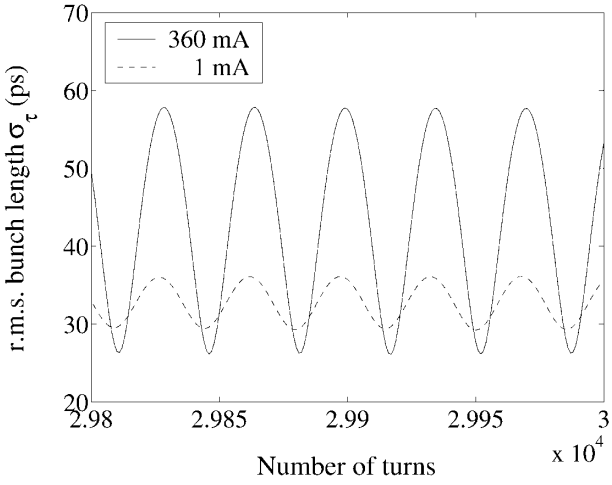

FIG. 16. Variation of the rms bunch length under phase modulation ($f_{\mathrm{mod}} = 45.36$ kHz, $\phi_{m0} = 0.028$ rad), which was obtained from a multiparticle tracking simulation. The calculated bunch lengths during the last 200 turns among the 30 000 turns are shown for beam currents of 360 mA (solid line) and 1 mA (dashed line), respectively. Note that one synchrotron period corresponds to about 70 turns. An averaged bunch length is about 44 ps for the beam current of 360 mA.

excitation to the beam current was actually observed during our experiments.

The calculated variation of the rms bunch length under the phase modulation is shown in Fig. 16. Under both beam currents of 360 and 1 mA, the bunch length oscillates at twice the synchrotron frequency. Under the beam current of 360 mA, the simulation predicts a time-averaged bunch length of about 44 ps, which is about 1.4 times longer than the natural bunch length of 31 ps. This result seems to be roughly consistent with the experimental observation using the streak camera.

C. Beam lifetime

We try to explain here the observed behavior of the beam lifetime in the PF storage ring. The lifetime during the experiment (shown in Fig. 3) is summarized in Table II. We can consider that the beam lifetime in the PF storage ring is mainly determined by both the beam-gas scattering process and the Touschek effect.

The lifetime ($\tau_{\rm gas}$) due to the scattering of the beam with a single species of molecules is given by [10,11]

$$\frac{1}{\tau_{\rm gas}} = \sigma_T d_m c\,, \tag{28}$$

where σ_T is the total cross section of the scattering processes that causes the loss of particles, d_m is the molecular density, and c is the speed of light. If the residual gas is a mixture of gases, $(\tau_{\rm gas})^{-1}$ is given by the sum of the contributions from all molecular species. We usually consider three kinds of scattering processes: the Coulomb scattering with nuclei, the emission of Bremsstrahlung, and the Møller scattering with orbital electrons. We can estimate that the residual gas in the PF storage ring is composed of H_2 gas of about 63%, CO gas of about 32%, CH_4 and CO_2 gases of about 1.6% each, and a few other gases [12]. Using them together with other parameters of the PF storage ring we can estimate the lifetime $\tau_{\rm gas}$ during the experiment to be about 195 h, under the phase modulation. Under no phase modulation, the estimated lifetime is about 10% shorter than this due to a slightly higher pressure. This difference in the pressure was, possibly, due to a difference in the parasitic mode loss.

TABLE II. Summary of the beam lifetime during the experiment. The number of bunches was 280 with almost equal filling.

Phase modulation[a]	On	Off
Beam lifetime	36 h	22 h
Average ring pressure[b]	7.4×10^{-8} Pa	8.2×10^{-8} Pa
Beam current	361 mA	358 mA

[a] $f_{\rm mod} = 48.1$ kHz, $\phi_{m0} = 0.028$ rad (3.2° peak to peak).
[b] Three times the average reading of the gauges.

On the other hand, the loss of the stored electrons due to the scattering process inside the bunch is called the Touschek effect [13]. The lifetime due to this effect is given by [14]

$$\frac{1}{\tau_{\rm Tous}} = \frac{N_0 r_e^2 c}{8\pi\sigma_x\sigma_y\sigma_z\gamma^2(\frac{\Delta E}{E})^3_{\rm max}} D(\xi)\,, \tag{29}$$

where $\tau_{\rm Tous}$ is the Touschek lifetime, N_0 is the number of particles in a bunch, r_e is the classical electron radius, $(\Delta E/E)_{\rm max}$ is the rf bucket height, and σ_x, σ_y, σ_z are the horizontal, vertical, and the longitudinal rms beam sizes, respectively. The function $D(\xi)$ is a slowly varying function of ξ, which is given by

$$D(\xi) = \sqrt{\xi}\left\{-\frac{3}{2}e^{-\xi} + \frac{\xi}{2}\int_\xi^\infty \frac{\ln u e^{-u}}{u}\,du + \frac{1}{2}(3\xi - \xi\ln\xi + 2)\int_\xi^\infty \frac{e^{-u}}{u}\,du\right\}, \tag{30}$$

with ξ being defined by

$$\xi = \left\{\frac{m_e c}{\sigma_{p,x}}\left(\frac{\Delta E}{E}\right)_{\rm max}\right\}^2. \tag{31}$$

Here, $\sigma_{p,x}$ is the rms spread of the horizontal particle momenta and m_e is the electron mass.

In the PF storage ring, the coupling coefficient for the horizontal and vertical motions is estimated to be about 1% [15]. We assume that the beam emittance and the energy spread are determined only by the synchrotron radiation effects, although this is not always the case in the experiments. Using the ring parameters in Table I, together with the design optical functions, $(\tau_{\rm Tous})^{-1}$ can be estimated at different locations in the ring. By averaging this result over the ring, we estimate the Touschek lifetime to be about 46 h under a beam current of 360 mA with 280 bunches. As a reference, we give some of the estimated parameters: $\langle\sigma_x\rangle = 0.49$ mm, $\langle\sigma_y\rangle = 0.06$ mm, $\sigma_z = 9.4$ mm, $N_0 = 5.0 \times 10^9$, $\xi = 5.6 \times 10^{-4}$, and $D(\xi) = 0.13$. Note that this estimation is based on several assumptions.

When the phase modulation is applied, the quadrupole oscillation of the bunch is excited; as a result, the average bunch length becomes long. Since the Touschek lifetime is proportional to the bunch length, we expect that the Touschek lifetime is elongated by the same factor as the bunch length. The multiparticle simulation in Sec. III B predicted the bunch lengthening by the factor of 1.4 for our experimental conditions ($I_0 = 360$ mA, $\phi_{m0} = 0.028$ rad). Thus, we estimate the Touschek lifetime to be about 65 h under the phase modulation. We have neglected here a possible small increase in the transverse beam size due to an increase in the energy spread.

Table III gives a summary of the above estimations. The estimated total beam lifetimes agree with the experimental results within a factor of 2. We predict that

TABLE III. Estimated beam lifetime for the experimental conditions in Table II.

Phase modulation	On	Off
τ_{gas}	195 h	180 h
τ_{Tous}	65 h	46 h
τ_{total} [a]	49 h	37 h

[a]Total beam lifetime.

the total beam lifetime will be improved by a factor of about 1.3 by applying the phase modulation, while the experiment resulted in a factor of 1.6. Thus, the improvement in the lifetime due to phase modulation can be explained by this model, at least to a certain measure of its quantity.

D. Cure for the longitudinal coupled-bunch instability

It is noted in Sec. II that the longitudinal coupled-bunch instability could be eased by applying rf phase modulation at a frequency of twice the synchrotron frequency. We briefly discuss here how the longitudinal coupled-bunch instability is affected by the phase modulation.

When there are cavitylike structures in the storage ring, the stored bunches can leave electromagnetic fields behind themselves. Such fields can couple the motions of different bunches, which can lead to the growth of such coupled oscillations. This phenomenon is called the coupled-bunch instability; the nature of such an instability has been understood very well [16–19]. The longitudinal coupled-bunch instability is driven by a longitudinal beam-coupling impedance of a resonant structure. Suppose that there are M equally spaced bunches; the instability arises if the shunt impedance of the structure is large enough, and the resonant frequency (f_{res}) is close to one of the following frequencies:

$$f_{\mathrm{res}} \approx mMf_r + \mu f_r + f_s\,, \tag{32}$$

where f_r is the revolution frequency, f_s is the synchrotron frequency, m is an arbitrary integer, and μ ($= 0, 1, \ldots, M-1$) is the integer called the coupled-bunch mode number. In such a case, each particle among the nth bunch will execute the following synchrotron oscillation:

$$\tau_n \sim \tau_{n0} e^{\alpha^{(\mu)} t} \cos(\omega_s^{(\mu)} t - \psi_n^{(\mu)})\,, \tag{33}$$

where $\alpha^{(\mu)}$ is the growth rate for the μth mode of oscillation, $\omega_s^{(\mu)}$ is the perturbed synchrotron frequency, and $\psi_n^{(\mu)}$ ($= 2\pi\mu n/M$) is the oscillation phase for the nth bunch.

Suppose that a certain particle executes a synchrotron oscillation given by

$$\tau = \tau_0 \cos(\omega_s t - \psi_0)\,. \tag{34}$$

The following quantity is an invariant of the small synchrotron motion that is free from any external forces:

$$W = \frac{1}{2}(\dot{\tau}^2 + \omega_s^2 \tau^2)\,. \tag{35}$$

We consider how this W changes when a small phase modulation is applied. Omitting the damping term from Eq. (8), the equation of motion is given by

$$\ddot{\tau} + \omega_s^2\{1 + \epsilon\cos(2\omega_s t)\}\tau = 0\,. \tag{36}$$

Then, the average rate of change in W is given by

$$\left\langle \frac{dW}{dt} \right\rangle = -\frac{\epsilon\omega_s^3\tau_0^2}{4}\sin(2\psi_0)\,. \tag{37}$$

Because of the phase modulation, the oscillation reduces ($\dot{W} < 0$) if the initial phase holds the condition of $\sin(2\psi_0) > 0$, and the reverse also holds.

Suppose that the synchrotron oscillation of a particle in the nth bunch is driven by the coupled-bunch instability, as given in Eq. (33). Then, applying the phase modulation will prevent, or promote, the oscillation according to the sign of $\sin(2\psi_n^{(\mu)})$. Considering this effect for each bunch, it will change the eigenmodes of the coupled-bunch oscillation. This is considered to be one of the possible mechanisms determining how the phase modulation affects the coupled-bunch instability.

As another approach, we studied the effect of phase modulation on the coupled-bunch instability by using a computer simulation. We used a simulation technique similar to that by Kubo [20]. Since we have not identified the impedance sources in the PF storage ring that cause the longitudinal instability, we assumed a model impedance in the simulation. We assumed a single resonance having the following parameters: $f_{\mathrm{res}} = 1003.428\,45$ MHz [i.e., the case of $m = 2$, $M = 312$, and $\mu = 2$ in Eq. (32)], $R_{\mathrm{sh}}/Q = 100\Omega$, and $Q_L = 2000$. With these parameters, the threshold current of the instability is predicted to be about 30 mA. In the simulation, each bunch was simply modeled by a single macroparticle. Then, we tracked the motion of such macroparticles while taking account of the interaction of the particles with the voltages induced in the resonant structure and in the accelerating cavity. We treated these beam-induced voltages in a similar way to that of the beam-loading effect as described in Sec. III B.

The results of the simulations are shown in Fig. 17, where the time displacements of the first bunch among the 312 bunches are plotted. Figures 17(a) and 17(b) show the cases with and without applying phase modulation, respectively. In the first case [Fig. 17(a)], the synchrotron oscillation grows exponentially with a growth rate similar to an analytical estimation. After the amplitude has reached its maximum, the amplitude reduces rapidly and this process is repeated. In the second case [Fig. 17(b)], the oscillation initially grows faster than in the first case due to the phase modulation, but the maximum amplitude of the oscillation is reduced. This reduction in the saturation amplitude would be one of the mechanisms which

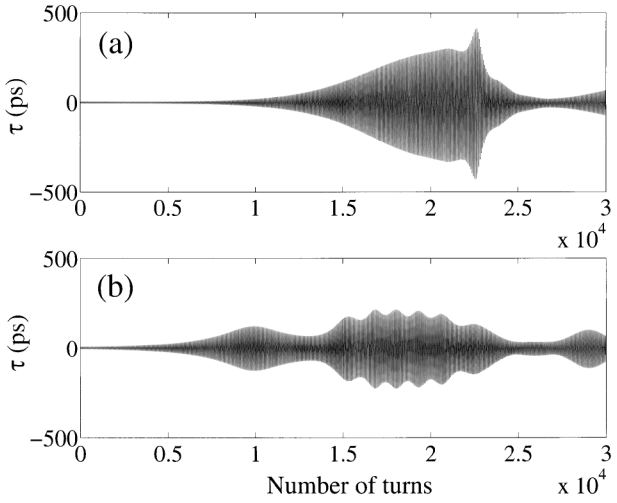

FIG. 17. Simulation results on the longitudinal coupled-bunch instability for the case (a) without applying phase modulation and the case (b) with phase modulation ($f_{\mathrm{mod}} = 45.36$ kHz, $\phi_{\mathrm{mod}} = 0.028$ rad). The time deviations of the first bunch are plotted over 30 000 turns. Assume that all of the bunches are filled uniformly with the beam current of 100 mA. Assume the following resonance for the impedance source: $f_{\mathrm{res}} = 1003.428\,45$ MHz, $R_{\mathrm{sh}}/Q = 100\Omega$, and $Q_L = 2000$. Other parameters are taken from Table I. The initial conditions for τ and δ of the bunches are assumed to be randomly distributed with maximum deviations of ± 10 ps (for τ) and $\pm 2 \times 10^{-4}$ (for δ), respectively.

eased the longitudinal instability in the experiments. Figure 18 shows another plot from the same simulation, in which the distribution of the bunches after 20 000 turns is plotted in phase space. It can be seen that the bunches lie on an ellipse in the case with no phase modulation (indicated by crosses), but the distribution is largely distorted from the ellipse in the case with phase modulation (indicated by dots).

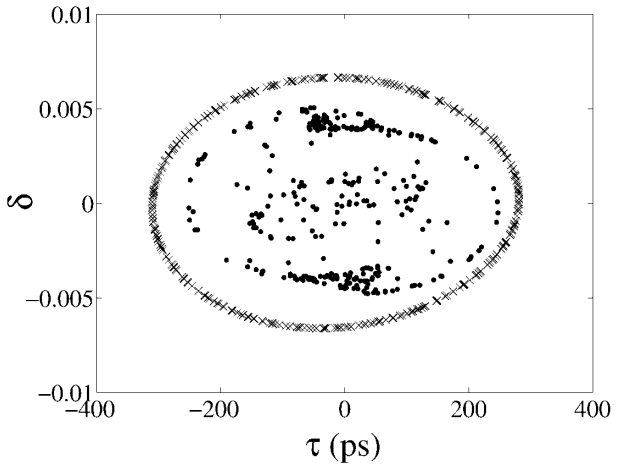

FIG. 18. Distributions of the bunches in phase space on the way (at 20 000th turn) to the growth of the instability. Each bunch is indicated by a cross (under no phase modulation) or a dot (under phase modulation), respectively. The assumed conditions are the same as in Fig. 17.

In the above-mentioned simulation, we ignored the motion of the particles inside the bunch. It should be noted that this "internal" motion of the particles may cause a further reduction of the oscillation amplitude when phase modulation is applied.

IV. CONCLUSIONS

We have shown both experimentally and theoretically that by applying a small phase modulation to the accelerating voltage at twice the synchrotron frequency, the quadrupole mode of longitudinal oscillation of the bunches can be excited through a parametric-resonance process. This makes the average bunch length long and results in the long Touschek lifetime. At the same time, the longitudinal coupled-bunch instability can be considerably suppressed. Both of them were found to be very useful for our operations.

We have been using this technique for routine operations since May, 1999. By optimizing the conditions of phase modulation, we have recently (in February, 2000) achieved a very long lifetime of 50 h with a beam current of 400 mA under daily operations. Also, the longitudinal coupled-bunch instability has been considerably suppressed using this technique. Although the phase modulation increases the beam energy spread to a certain extent, the overall beam quality is improved as the result of suppressing the longitudinal instability.

ACKNOWLEDGMENTS

We wish to thank M. Katoh and Y. Hori for useful discussions and Masanori Kobayashi for encouraging us in this work. We are also grateful to M. Tadano for preparing useful software for the technique used in our operations.

[1] KEK Photon Factory Activity Report, 1998, edited by Y. Hori *et al.* (unpublished).
[2] M. Katoh *et al.*, J. Synchrotron Radiat. **5**, 366 (1998).
[3] M. Katoh *et al.*, in *Proceedings of the Sixth European Accelerator Conference, Stockholm, 1998* (Institute of Physics Publishing, Bristol, Philadelphia, 1998), pp. 590–592.
[4] M. Izawa *et al.*, J. Synchrotron Radiat. **5**, 369 (1998).
[5] KEK Photon Factory Activity Report, 1983/84 (unpublished), pp. IV9–IV10.
[6] L. D. Landau and E. M. Lifshitz, *Mechanics* (Pergamon Press, Oxford, 1976), 3rd ed.
[7] M. Toda, *Theory of Vibrations* (Bai-fu-kan, Tokyo, 1968), in Japanese.
[8] K. Hirata, KEK Internal Report No. 85-3 (unpublished), in Japanese.
[9] P. B. Wilson, in *Physics of High Energy Particle Accelerators,* edited by R. A. Carrigan, F. R. Huson, and

M. Month, AIP Conf. Proc. No. 87 (AIP, New York, 1982), pp. 450–563.
[10] S. Kamada, KEK Report No. KEK-79-20 (unpublished), pp. 1–10, in Japanese.
[11] H. Wiedemann, *Particle Accelerator Physics* (Springer-Verlag, Berlin, 1993).
[12] Y. Hori and M. Kobayashi, Vacuum **47**, 621 (1996).
[13] C. Bernardini *et al.*, Phys. Rev. Lett. **10**, 407 (1963).
[14] J. Le Duff, in *Proceedings of the CERN Accelerator School, Second Advanced Accelerator Physics Course, Berlin, 1987*, edited by S. Turner (CERN, Geneva, 1989); CERN Report No. CERN 89-01, pp. 114–130.
[15] M. Katoh and T. Mitsuhashi, in Proceedings of the 12th Symposium on Accelerator Science and Technology, Wako, Japan, 1999 (unpublished).
[16] C. Pellegrini and M. Sands, SLAC Report No. PEP-258 (unpublished).
[17] H. Kobayakawa, Y. Yamazaki, Y. Kamiya, and M. Kihara, Jpn. J. Appl. Phys. **25**, 864 (1986).
[18] K. A. Thompson and R. D. Ruth, in *Proceedings of the 1989 IEEE Particle Accelerator Conference, Chicago, 1989* (IEEE, Piscataway, NJ, 1989), pp. 792–794.
[19] A. W. Chao, *Physics of Collective Beam Instabilities in High Energy Accelerators* (Wiley, New York, 1993).
[20] K. Kubo, in *Proceedings of the 1991 IEEE Particle Accelerator Conference, San Francisco, 1991* (IEEE, Piscataway, NJ, 1991), pp. 1833–1835.